X-622-69-195
PREPRINT

NASA TM X-63546

EVALUATION AND CALIBRATION OF SOME ENERGY SOURCES FOR THE VISIBLE AND NEAR INFRARED REGIONS OF THE ELECTROMAGNETIC SPECTRUM

A. W. McCULLOCH
J. T. McLEAN
E. I. MOHR

MAY 1969

GODDARD SPACE FLIGHT CENTER
GREENBELT, MARYLAND

X-622-69-195

EVALUATION AND CALIBRATION OF SOME ENERGY SOURCES FOR THE VISIBLE AND NEAR INFRARED REGIONS OF THE ELECTROMAGNETIC SPECTRUM

A. W. McCulloch
J. T. McLean
NASA/GSFC

E. I. Mohr
Columbia Union College
Consultant to NASA/GSFC

May 1969

GODDARD SPACE FLIGHT CENTER
Greenbelt, Maryland

LIST OF FIGURES

EVALUATION AND CALIBRATION OF SOME ENERGY SOURCES FOR THE VISIBLE AND NEAR INFRARED REGIONS OF THE ELECTROMAGNETIC SPECTRUM

I. INTRODUCTION

The concept of energy is a simple one: It is either work which is potentially available, or which has been done. Its dimensions are $(\text{length})^2(\text{mass})/(\text{time})^2$. There are internationally accepted standards of length, mass and time. These can be measured with a great deal of precision, but the measurement of energy leaves much to be desired.

The measurement of radiant energy involves a number of fundamental phenomena related to its production, its propagation through space and its effect on energy sensing devices. This report deals with several energy sources which have been examined experimentally.

II. SMALL AREA ENERGY SOURCES

A. THE BLACKBODY

When a substance is heated, it emits radiation. If the temperature is high enough, this includes radiation in the visible region. If a radiation field is enclosed by matter at a given temperature, energy will be interchanged between the field and matter. A state of equilibrium will be reached in which the field has a specific distribution of energy as a function of frequency or wavelength. The distribution depends only on the temperature and not on the nature of the material enclosing the field. This type of radiation is called blackbody radiation since the perfect radiator is also a perfect absorber and if cold would appear black. The spectral distribution of blackbody radiation is given by Planck's radiation law. This law gives the distribution which exists in an internal cavity of a body at a given temperature. The same distribution would prevail for a body which is a perfect absorber and hence a perfect radiator.

The total radiation of a body is given by the Stefan-Boltzmann equation:

$$E = \sigma T^4 . \tag{1}$$

Thus one must know the temperature accurately in order to know the energy emitted by the source. For a gray body, assuming constant emissivity, ϵ, this becomes

$$E = \epsilon \sigma T^4 . \tag{2}$$

Hence a change in total radiation may be produced either by a change in emissivity, or by a change in temperature. For equal percentage changes in T or ϵ, the total radiation will change four times as much with temperature as with emissivity. At ambient temperature (300°K) a change in emissivity of one percent produces the same change in total radiation as a change in temperature of 3/4°. (Ref. 1).

Two commercially made sources whose emissivities are claimed to be .99 ± .01 independent of wavelength have been used in the investigations being reported. Both are designed to operate at a maximum temperature of 1000°C. One of these was made by Barnes Engineering Co. It has a series of apertures ranging in diameter from 0.2564" down to .0081". The sizes are chosen to provide equal area increments. The second blackbody was made by Infrared Industries. It has a variable aperture, with a maximum available diameter of 0.6".

Both of these blackbodies have the disadvantage of not having a provision for maintaining the face plate (and aperture) at ambient temperature. The Infrared Industries blackbody is somewhat better in this respect than the Barnes source since it has a double face plate, the inner-one being made of asbestos. Thus its temperature is only ten to fifteen degrees above ambient temperature.

The cavity temperature of the blackbodies was checked by means of a platinum-platinum plus 13% rhodium thermocouple and also by means of an optical pyrometer in the case of temperatures above 800°C. The apertures were measured by means of a measuring microscope.

It is obviously advantageous to use black body radiation for calibration purposes since, if one has a reliable determination of its temperature and aperture size, the total as well as the spectral distribution of the emitted energy is well known. A disadvantage is that the total energy of the currently available sources is somewhat low due to an upper temperature of 1000°C. This problem can be corrected in later investigations when a recently acquired 3000°C blackbody is placed in operation.

B. TUNGSTEN RIBBON FILAMENT LAMPS

One standard of spectral radiance often used is a tungsten ribbon filament lamp. An important advantage of this type of source is that it can be operated at high temperatures. A special type, available from the National Bureau of Standards (Ref. 2), is calibrated with reference to primary standard lamps or to a blackbody at known temperature. This type of lamp normally operates at about 6 volts with a current of 25, 30, or 35 amperes depending on the desired spectral region. To insure that the lamp output covers all wavelengths in this range, it is provided with a fused quartz window.

The data supplied by the N.B.S. gives the spectral radiance over a wavelength range from 0.5 microns to 2.6 microns. In order to use the lamps as a secondary standard of total radiance, it is necessary to extend the values of the spectral radiance somewhat into the ultraviolet and especially into the infrared region.

For this extrapolation one may use values of N_λ, the spectral radiance of a blackbody from tables by Pivovonsky (Ref. 3), ϵ_λ, the spectral emissivity of tungsten from data by de Vos (Ref. 4), and τ_λ, the spectral transmissivity of quartz. Using these values, tables were prepared for the computed values of $N_\lambda \epsilon_\lambda \tau_\lambda$ at narrow wavelength intervals for the following temperatures: 1800°, 2000°, 2200°, 2400°, 2600°, 2800°, 3000° (Kelvin). By comparing the computed values of $N_\lambda \epsilon_\lambda \tau_\lambda$ with the calibration data supplied by the N.B.S. it was possible to assign a temperature to the tungsten ribbon. Using the assigned value of the temperature of the ribbon, the spectral radiance in the ultraviolet and infrared were obtained from the tables of values of $N_\lambda \epsilon_\lambda \tau_\lambda$ by interpolation.

The total effective radiance, $\overline{N}$, radiated by one square millimeter per unit solid angle normal to its surface in the specified wavelength region was determined by evaluating the expression

$$\overline{N} = \sum_{0.2\mu}^{4.8\mu} N_\lambda \epsilon_\lambda \tau_\lambda \Delta\lambda \, . \tag{3}$$

This value, when multiplied by the area of the tungsten ribbon as calculated from measurements made with a measuring microscope, gave the total radiant intensity, J, in watts per steradian, emitted by the ribbon normal to its surface as viewed through the quartz window.

While there is some uncertainty in the values obtained by this method, it should not be large since the data obtained by extrapolation only adds a small amount (less than 10%) to the total energy emitted through the quartz windows of the three specific lamps studied. Hence the probable error in the additional energy will certainly be less than the ±5% maximum error averaged over the entire spectral range claimed by the N.B.S. for their calibration of the tungsten ribbon lamps.

The above procedure was initially worked out by M. P. Thekaekara of Goddard's Test and Evaluation Division. It was extended and used by E. I. Mohr. A number of lamps in the T. and E. Division and the lamps EU235 (at 35 amps), E185 (at 30 amps) and E185 (at 25 amps) of the Planetary Radiations Branch were evaluated for total radiance using this method during the winter of 1963-64.

C. QUARTZ-IODINE LAMPS (STANDARDS OF SPECTRAL IRRADIANCE)

Quartz-iodine lamps (Ref. 5 and Ref. 6) have several characteristics which make them superior to conventional tungsten lamps. Because of the presence of a trace of iodine gas in the bulb acting as a "transport mechanism" to return the evaporated tungsten to the filament, it may be operated at a much higher temperature than conventional lamps. In addition, the resistance of the quartz envelope to high temperatures makes it possible to make a more compact lamp for a given power rating. Because of its convenient size and other advantages as noted above, it is quite suited as a standard of spectral irradiance (Ref. 7).

As with the ribbon filament sources, in order to use the quartz-iodine lamps as secondary standards of total radiance, it is necessary to extend the values of the spectral irradiance provided by the N.B.S. into the infrared region by extrapolation. In addition, for wavelengths greater than 3 microns, the hot quartz envelope begins to contribute a significant amount of emitted energy to the total. This problem was investigated by E. I. Mohr under the direction of M. P. Thekaekara during the winter of 1964-1965. A complete report of this work is given in the 1965 Summer Workshop Report (Ref. 8). A further evaluation of those results is presented in the next section.

D. THE QUARTZ-IODINE LAMP AS A STANDARD FOR TOTAL RADIANCE: A REEVALUATION

1. General

A report on the studies made on the applicability of quartz-iodine lamps as secondary standards of total radiance was referred to above (Ref. 8). In this study, the energy emitted by the envelope of the quartz-iodine lamp was evaluated by obtaining the product of the spectral radiance of a blackbody and the emissivity of fused quartz. This emissivity was based on the work reported by Pirani (Ref. 9). More recent data reported on the emissivity of fused quartz (Ref. 10 and Ref. 11) indicate that it is not as high as the values given by Pirani. The values obtained from these references are tabulated in Table I. These new values for the emissivity of fused quartz as well as a different value of the temperature, described below, were used to recalculate the total radiance of the quartz envelope of the 1000-watt quartz-iodine lamp.

Table I

Spectral Emissivity of Fused Quartz

λ	ϵ	λ	ϵ	λ	ϵ
3.0	.02				
3.2	.07	5.5	.96	11	.83
3.4	.11	6.0	.95	12	.84
3.6	.16	6.5	.94	13	.80
3.8	.24	7.0	.93	14	.99
4.0	.44	7.5	.84	15	.99
4.2	.70	8.0	.75	16	.99
4.4	.83	8.5	.66	17	.99
4.6	.92	9.0	.45	18	.95
4.8	.97	9.5	.64	19	.98
5.0	.96	10.0	.76	20	.85

The method used to estimate the temperature of the quartz envelope is described in Reference 8. This method was found to be prone to error, so an attempt has been made to measure directly the temperature of the lamp support and of the envelope. For this purpose a thermocouple composed of platinum-platinum plus 13% rhodium was used. The hot junction was firmly held against the surface to be measured by means of a spring clamp. The temperatures measured on different parts of the lamp support varied between 360°K and 390°K. In order to determine the temperature of the quartz envelope, the spring clamp was used to press a strip of teflon against the hot junction of the thermocouple to ensure good contact between the envelope and the thermocouple. The temperature was found to be 660°K at the lower end of the lamp (mounted vertically) and 705°K at the upper end. These values may well be too high since the teflon reduces the loss by radiation and convection.

It was not possible to use the thermocouple to measure the temperature at the midpoint of the envelope. A private communication regarding investigations of the temperature of quartz-iodine lamps in an industrial laboratory indicated that a rather high temperature gradient exists from the center to the end of the lamp. Thus one ought to divide the length of the lamp into short sections, each at a known temperature and determine the summation of $N_\lambda \epsilon_q \Delta A$ over the range 3.0 to 20 microns for each section. ΔA is an incremental area of a particular section. The total radiance of the envelope would be obtained by adding the output of all the sections. An alternate method would be to evaluate the output for some "average" temperature. This was the approach taken assuming 700°K as a reasonable average value. The total radiant intensity of the envelope, $\bar{J}_e$, was obtained by evaluating the sum

$$\bar{J}_e = \sum_{3.0}^{20} N_\lambda \epsilon_{q\lambda} A \Delta\lambda \tag{4}$$

where N_λ is the spectral radiance of a black body at 700°K, $\epsilon_{q\lambda}$ the emissivity of the quartz, A the area of the longitudinal section, and $\Delta\lambda$ the wavelength increment. The resulting value for the total radiance of the envelope is only 41% of the value reported in Reference 8.

The investigations reported in Reference 8 made use of the ratio

$$R = N_\lambda' / N_\lambda \epsilon_{w_\lambda} \tau_q \tag{5}$$

in order to evaluate the temperature of the tungsten coil and obtain the radiance of the coil for wavelengths greater than 2.5 microns. N_λ' is the spectral radiance of the standard lamp, N_λ the spectral radiance of a blackbody at a given temperature, $\epsilon_{w\lambda}$ the emissivity of the tungsten and τ_q the transmittance of the quartz. This ratio shows a sharp increase from a value of about 2 to a value of 3 in the range 2.1 to 2.5 microns. This slope, as reported in Reference 8, was used to obtain the radiance of the lamp for the range 2.6 to 4.8 microns at which point the quartz becomes opaque. Theoretically it would seem that this ratio should remain constant if the emissivity of the tungsten were known accurately. Thus a constant ratio was assumed and taken as equal to the value of 2.0 microns. The total effective radiance of the coil, $\bar{N}_\ell$, in the range 2.6 to 4.8 microns was obtained by the equation

$$\bar{N}_\ell = \sum_{2.6}^{4.8} R N_\lambda \epsilon_{w_\lambda} \tau_q \Delta\lambda \tag{6}$$

where R is the above mentioned ratio. This gave a decrease in the radiance of the tungsten to 84.5% of its previous value in the case of lamp QM-B, and a decrease to 81.9% in the case of lamp QM-95.

As a result of the decrease in the flux due to the radiance of the coil in the range 2.6 to 4.8 microns and of the quartz envelope the radiant flux in watts per steradian decreased to 92.6% of the value obtained by the former method in the case of lamp QM-B, and to 92.2% in the case of lamp QM-95.

2. Angular Distribution of Flux Around the Lamp

To determine this distribution, the quartz-iodine lamp QM-B was mounted with its axis vertical and rotated about the vertical axis through 360°. A water-cooled thermopile designated 4928A was mounted on the same optical bench at a distance of 70 cm and used to measure the intensity of the flux emitted normal to the lamp. This was measured for every 15° of rotation of the lamp. The flux was found to remain approximately constant.

The lamp was then mounted with its axis in a horizontal direction and rotated about a vertical axis through its center while the thermopile remained at 70 cm. The intensity of the flux was measured for every 10° while the lamp was rotated through 180° or from the position in which one end of the lamp was toward the detector until the opposite end pointed toward the thermopile. These data were plotted on polar coordinate paper and a Rousseau diagram was constructed by use of this graph. The average height of the Rousseau diagram was multiplied by 4π to obtain the total power radiated by the lamp in all directions.

3. Input Power Versus Total Flux Emitted by the Lamp

The quartz-iodine standard lamp used in our studies operates at 8.30 amperes. This current was monitored by a standard Weston ammeter Model 326, No. 3112. The voltage across the lamp was measured by means of a standard Weston voltmeter Model 326, No. 3113. The product of the two values gave the input into the lamp in watts. Table II gives the power input into three standard lamps and the corresponding power output of the same lamps as determined by means of the angular distribution and the Rousseau diagram, assuming that the three standard lamps have the same angular distribution as that of lamp QM-B.

From the dimensions of the leads and the ceramic ring around the leads and the measured and estimated temperature differences, it was estimated that the loss by conduction is about 0.3 watt. No estimate has been made in regard to the energy loss from the lamp due to air convection.

Table II

Comparison of Input Power and Radiant Flux

Lamp	Input Power	Output Power	Difference	% Difference
QM-95	889.3	876.0	-13.3	-1.50
EPI-1154	879.4	865.4	-14.4	-1.64
EPI-1155	904.3	891.3	-13.0	-1.44

4. Discussion of the Results

The average output of the three standard lamps is 13.6 watts or 1.53% less than the power input. As stated above, conduction losses represent only about 2.5% of this difference. A portion of this difference may be due to energy radiated by the lamps at wavelengths greater than 20 microns, although it most likely represents only a fraction of this difference. It is quite probable that the greater portion of this difference may be due to a loss of energy by the lamps due to convection currents. However, no evaluation of these convection losses is possible at this time.

E. A NEW STANDARD OF TOTAL IRRADIANCE

The National Bureau of Standards has long been issuing a standard of total irradiance in the form of a 50 watt carbon filament lamp. The calibration of such lamps can be traced to Coblenz's original carbon filament standard established more than 50 years ago. With the current needs for standards of total irradiance of higher accuracy and greater intensity, the N.B.S. recently began to provide three sizes (100 watt, 500 watt, and 1000 watt) of tungsten filament lamps as standards of total irradiance (Ref. 12).

The use of the tungsten filament permits operation at color temperatures of the order of 2700°K to 2850°K in contrast to the color temperatures of 1800°K to 2000°K possible with the carbon-filament lamps.

In operation the new standards are shielded by a specially designed external triple metal (aluminum) shield and triple shutter. Each piece of the shutter and shield is blackened on the side away from the lamp and highly polished on the side toward the lamp. This shield is placed at the recommended distance of 25 cm from the lamp. It covers all of the lamp except for a narrow area of the bulb directly in front of the filament. In this way the long wavelength flux from the quartz envelope is reduced to a minimum and all surfaces visible to a detector viewing the source are near room temperature.

The N.B.S. has now authorized Eppley Laboratories to supply these lamps commercially.

F. WORKING STANDARDS

Secondary standard lamps, such as those which have been calibrated by the N.B.S., and more recently by the Eppley Laboratories, are expensive and have only a limited useful life. For this reason it is desirable to use these secondary standards for the purpose of calibrating working standards. Nathan J. Miller and E. I. Mohr used a 1000-watt NBS standard quartz-iodine lamp QM-95 to calibrate three 1000-watt quartz-iodine lamps designated as lamps QM-A, QM-B, and QM-C. The experimental procedure used and the spectral irradiance of these lamps was reported in the final report of the 1965 Summer Workshop Program (Ref. 13). For a calibration of this type, one ought to use several standard lamps. With the recent purchase of two additional 1000-watt quartz-iodine secondary standards, the Planetary Radiations Branch has three secondary standards available for any future calibration of this type.

III. THE SPHERICAL INTEGRATOR AS AN EXTENDED, DIFFUSE ENERGY SOURCE

A. THEORY OF THE SPHERICAL INTEGRATOR

The principle of spherical integration was proposed by Sumpner in 1892 (Ref. 14). He showed that if a source of light is placed inside a hollow sphere which is coated internally with a perfectly diffusing coat, the luminance of any portion of the surface due to the light reflected from the rest of the sphere is everywhere the same and is directly proportional to the total flux emitted by the source.

It is easy to show (Ref. 15) that the theoretical expression for this relation in terms of the reflectance ρ of the perfectly diffusing coat of the sphere wall due to an infinite number of reflections is given by

$$\Phi = \frac{F}{4\pi r^2} \times \frac{\rho}{1 - \rho} \tag{7}$$

where Φ is the total radiant flux reaching unit area of the spherical surface by reflection, F the total flux emitted by the source and r the radius of the sphere. In the derivation of Equation (7) it is assumed that ρ is constant, that the surface is a perfect diffuser, that the sphere is empty and that it has no ports. As a matter of fact, the reflectance ρ of the coating varies with wavelength. Moreover there is no perfect diffuser so that Lambert's cosine law does not hold accurately. In addition, the sphere has sources, shields and ports, all of which affect the total radiant flux. It has been shown that the error introduced into the calculated sphere output by the finite size of holes and samples may be as much as 25 percent (Ref. 16). Moreover, the spectral dependence of the reflection can modify considerably the spectral distribution of the flux streaming from the port of the sphere (Ref. 17). Thus the intensity is increased for wavelengths for which the reflectance is high and decreased for wavelengths for which the reflectance is low. In spite of these uncertainties one can calibrate the output of the sphere against a known standard for use as an absolute calibration source.

B. THE SPHERICAL INTEGRATOR

The spherical integrator of the Planetary Radiations Branch has a diameter of six feet (182.5 cm inside diameter). It consists of two hollow fiber-glass hemispheres, one of which is mounted on a rigid but movable framework. The second hemisphere is hinged to the first and held shut by a latch, thus permitting easy access to the interior. (See Figure 1.)

An exit port, with a diameter of 6.0 cm is located at the midpoint of the surface of the stationary hemisphere. This port allows ready access for the calibration of radiometers in the visible and near infrared regions and provides a sufficiently large field of view.

The inside of the sphere is covered with several coats of a white paint with a magnesium carbonate base manufactured by the Burch Co. This provides a satisfactory diffusing surface.

In order to hold to a minimum the size of the objects introduced into the sphere and also have some means of varying the intensity of the source, twelve quartz-iodine lamps, rated at 200 watts each, are mounted inside the sphere. These lamps are evenly spaced around the exit port on a circle with a radius of 18 inches. Small teflon shields, mounted in front of the lamps, prevent the flux

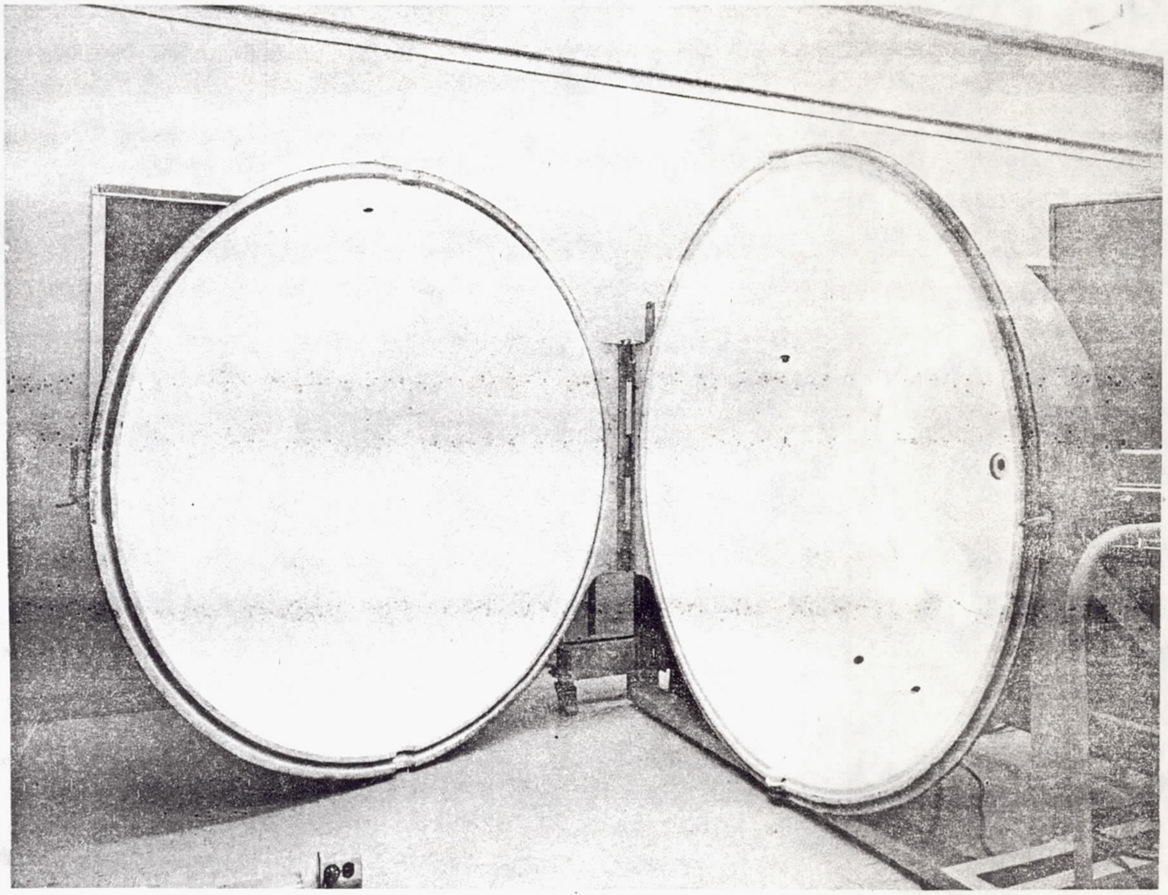

Figure 1. Stationary and Movable Hemispheres of the Six-Foot Spherical Integrator (Inside View)

from these lamps from reaching the port directly. Figure 2 is a view of the inside of the stationary hemisphere showing the position of the exit port surrounded by the twelve lamps.

A 3.8 cm diameter hole on top of the sphere, with a fan mounted over it, together with three holes of the same size in the bottom of the sphere provide a continuous flow of air through the sphere.

For a more complete description of the sphere in terms of the original position of ports and lamps see Reference 17.

C. POWER SUPPLY FOR THE INTEGRATOR LAMPS

The 200-watt quartz-iodine lamps require a 6.5 ampere current at approximately 30.3 volts. The lamps are operated in three banks of four lamps each. The four lamps in a given bank are in series.

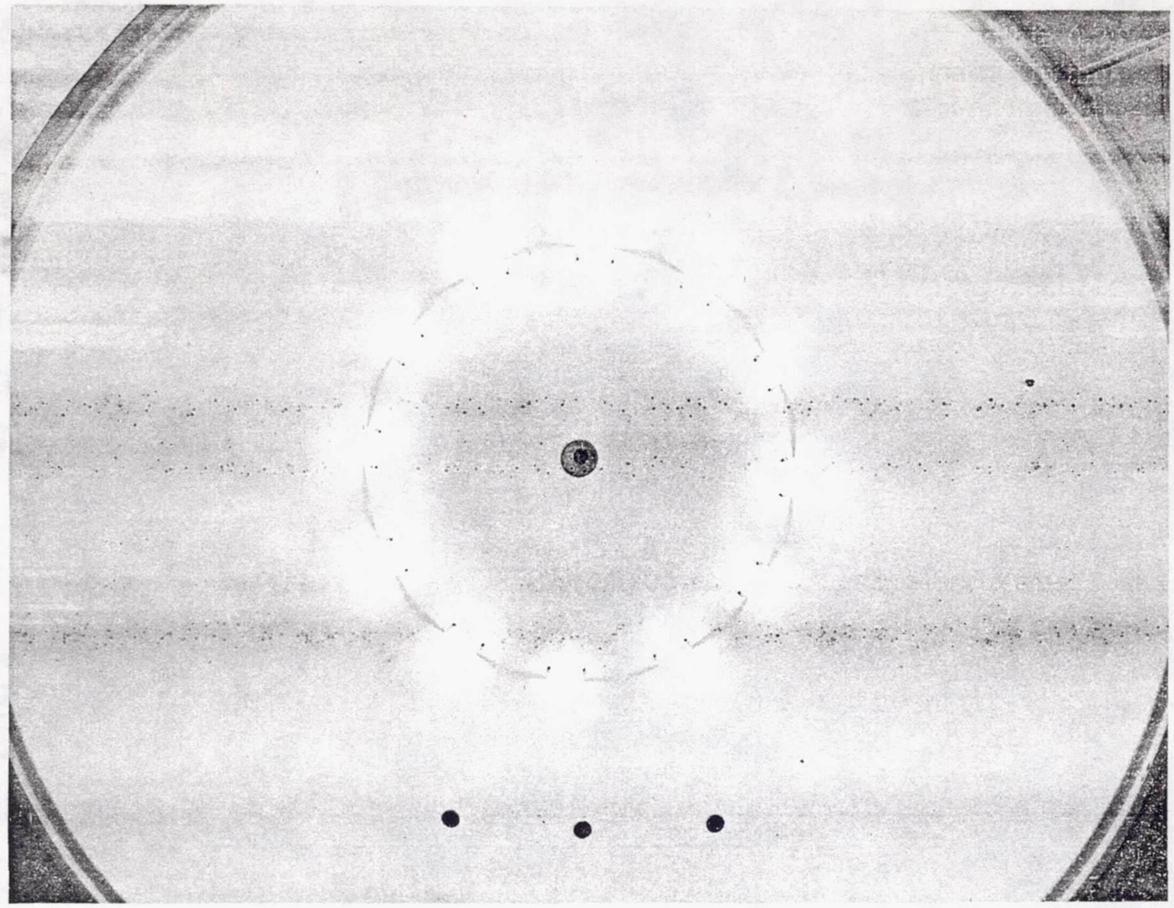

Figure 2. Inside View of the Stationary Hemisphere Showing the Location of the Exit Port and the Twelve Quartz-Iodine Lamps

Each bank of four lamps is operated by one of three power supplies. These power supplies are model 590-11 power supplies manufactured by Edgerton, Germeshausen & Grier, Inc. They have been specifically designed for use with various types of standard lamps. They are solid-state supplies designed to furnish programmed voltage and rms regulated current in preset combinations at power levels ranging from 2 to 1000 watts (1 to 50 amperes and 2 to 160 volts). The chopper stabilized square wave current is feedback regulated within 0.25% rms of the selected digital value for control of light output within 1%. In the present application, the power supplies were preset to provide a constant current of 6.5 amperes with a maximum available potential of 152 volts.

A switching arrangement allows any one or all of the lamps in a given bank to be turned off. Since this would result in a considerable decrease in load in the given bank, when one of its lamps is turned off, it is replaced at once by an equivalent load outside of the sphere. This load consists of a parallel combination of two ten-ampere, 200-watt Ohmite Dividohm Power Reistors located in the control rack so that the dissipated power does not contribute to the total flux in the sphere.

The circuit arrangement provides for constant monitoring of the voltage drop across each lamp separately, by means of a true RMS voltmeter. The D. C. output of this meter is fed into a digital volt-ohmmeter, which may be read to four significant digits. This continuous monitoring of the voltage permits the operator to note if and when the resistance of a given lamp begins to change. Since such a change is accompanied by a change in the lamp output and hence its intensity, the investigator knows that the particular lamp must be replaced by an equivalent lamp in order to keep the emittance of the sphere constant.

Figure 3 shows the six-foot integrator with the lamp power supply and the voltage monitoring equipment mounted in the rack to the left of the sphere. A Perkin-Elmer Double-Pass Monochromator Model 99, with a 16 inch integrator attached to it in front of the slit, is shown positioned in front of the exit port of the six-foot integrator. The power supply and recording equipment for the monochromator is mounted in the rack to the right of the sphere.

D. THE SPECTRAL REFLECTANCE OF THE BURCH SPHERE PAINT

The spectral reflectance of the sphere paint used in the preliminary calibration of the sphere was obtained by means of a Beckman DK-2A spectrophotometer and a Beckman IR-7 spectrophotometer (Ref. 17). The measurements were made by comparing the reflectance of the paint with that of freshly smoked magnesium oxide. The values which were obtained for the paint seemed rather high in comparison with those of magnesium oxide. At a later date, we were able to remeasure the reflectance of the paint using different instruments. The reflectance of the paint was compared with that of freshly smoked magnesium oxide in the range 0.2 to 2.5 microns by means of a Cary 14 double beam spectrophotometer. For the range 2.5 to 20 microns the reflectance of the paint was compared with a calibrated aluminum mirror as a standard by means of a Cary 90. The corresponding data are given in Table III and plotted in Figure 4. The data is shown only from 0.2 to 3.0 microns since beyond $3.0\,\mu$ the reflectance is essentially 0.

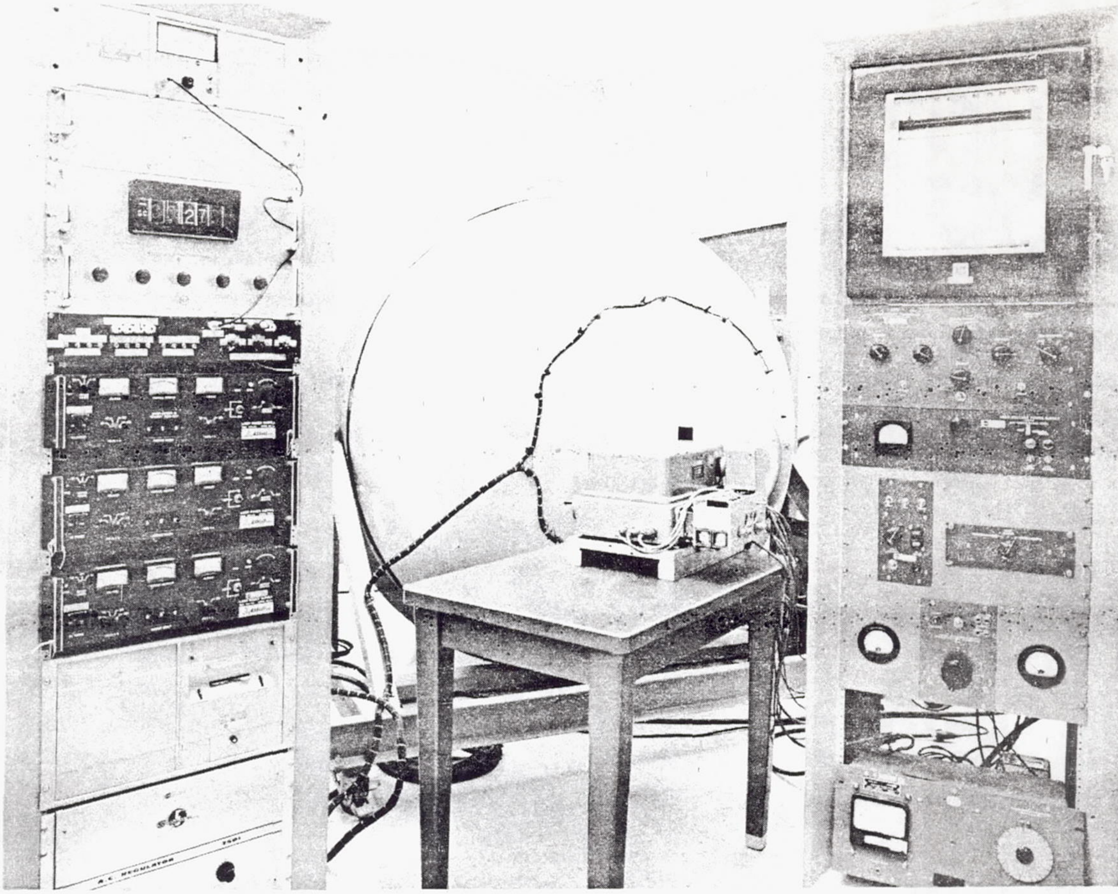

Figure 3. Outside view of the six-foot integrator. The rack to the left of the sphere contains the monitoring equipment and power supplies for the lamps. The monochromator, with the 16" sphere attached is located at the exit port of the large sphere. The rack to the right contains the amplifier and recorder for the monochromator.

E. RELATIVE SPECTRAL DISTRIBUTION OF THE SPHERE OUTPUT

Since the integrating effect of the sphere is influenced by the spectral dependence of the reflectance, it is necessary to compare the spectral distribution of the output with that from a standard of spectral radiance. Tests have shown that the number of lamps used in the sphere has no effect on the spectral distribution of the output within the limits of experimental accuracy (Ref. 17), hence twelve lamps were used to calibrate the sphere in order to get a satisfactory flux intensity.

The measurements of the spectral distribution of the sphere were made with a Perkin-Elmer Double-Pass Monochromator Model 99. The slit of the

Table III

Spectral Reflectance of Burch Sphere Paint

(λ in microns)

λ	ρ_λ	λ	ρ_λ	λ	ρ_λ
.20	.141	.45	.844	1.6	.803
.21	.145	.50	.874	1.7	.756
.22	.225	.55	.891	1.8	.740
.23	.336	.60	.903	1.9	.698
.24	.342	.65	.912	2.0	.645
.25	.426	.70	.914	2.1	.644
.26	.620	.75	.913	2.2	.654
.27	.735	.80	.913	2.3	.548
.28	.820	.90	.910	2.4	.490
.29	.769	1.00	.904	2.5	.460
.30	.626	1.1	.895	2.6	.443
.32	.627	1.2	.877	2.7	.291
.35	.705	1.3	.870	2.8	.059
.37	.755	1.4	.825	2.9	.025
.40	.802	1.5	.806	3.0	.048

monochromator was positioned as close to the port of the spherical integrator as possible. The slit width and gain were kept small in order to have the best resolution possible as well as a minimum amount of noise. For the wavelength range from 0.45 to 2.7 microns a Reeder thermocouple detector with quartz window was used. A photomultiplier detector 1P28 was used in the range from 0.32 to 0.7 microns. The spectral distribution for both ranges was automatically recorded by means of a Leeds and Northrup Speedomax G. Whenever it was necessary to change the slit width of the monochromator or the gain of the amplifier, a portion of the previously recorded spectral range was scanned again

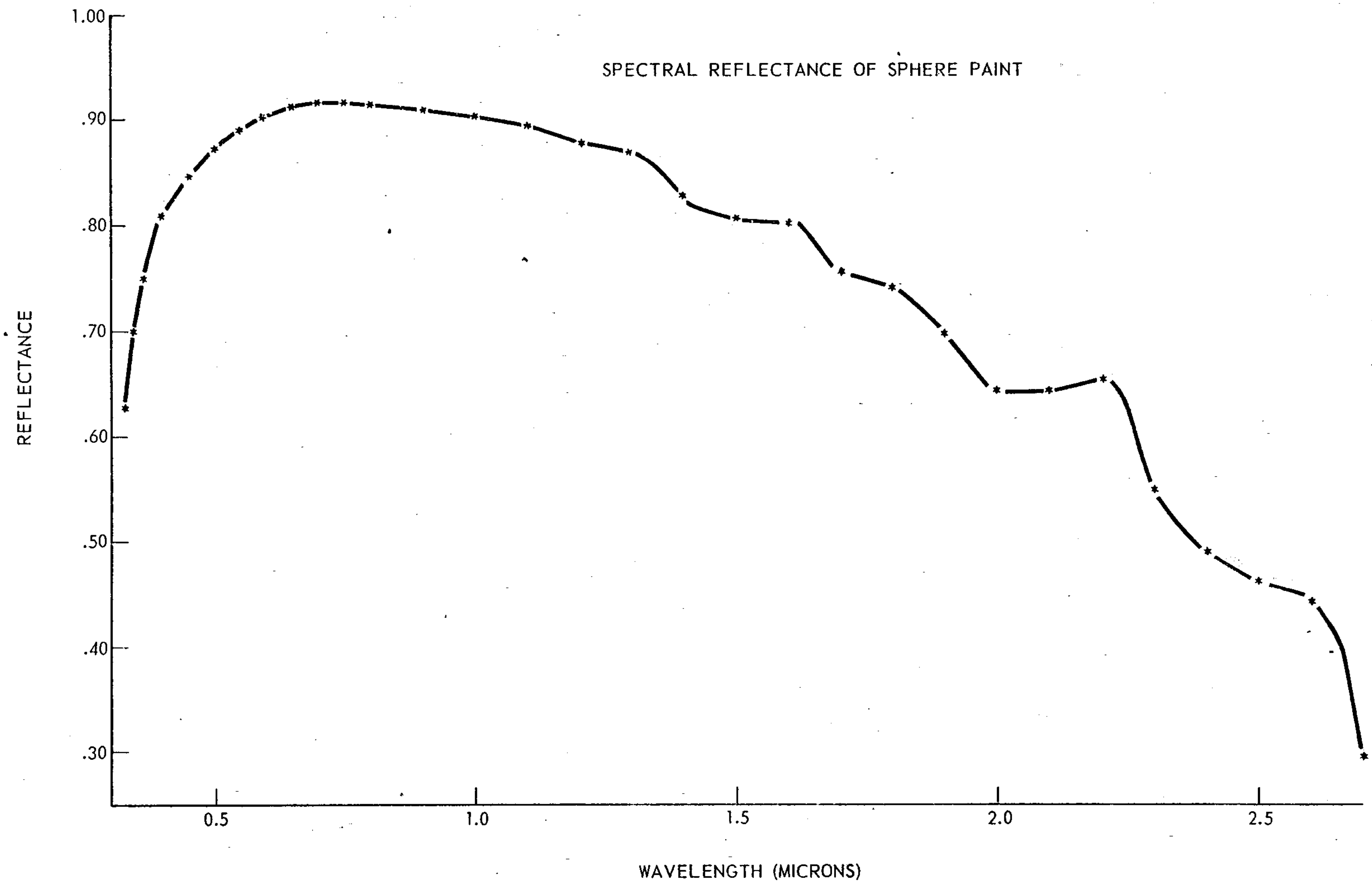

Figure 4. Spectral Reflectance of Burch Integrating Sphere Paint

in order to normalize all parts of the recorded range to the peak value of the deflection. This procedure was repeated several times to obtain the average value of the distribution.

In order to get the spectral distribution of the standard of radiance the N.B.S. calibrated 1000-watt quartz-iodine lamp QM-95 and the Eppley Laboratories lamps EPI-1154 and EPI-1155 were used. For a given trial one of these lamps was positioned about 2.4 meters in front of the slit of the monochromator and on a line with its axis. The spectral distribution of each lamp was obtained under the same conditions of slit width and amplifier gain as those which were used to get the spectral distribution of the output of the sphere and the results normalized as before.

The normalized recorder deflections $D_{s\,r\lambda}$ obtained for the output of the sphere were divided by the corresponding normalized recorder deflections $D_{l\,r\lambda}$ obtained for each of the standard lamps. This was done at one-tenth micron intervals or less over the entire spectral range which was scanned. This gave the relative ratios of the spectral distribution of the sphere and of a specific lamp. These ratios $k_{r\lambda} = D_{s\,r\lambda}/D_{l\,r\lambda}$ were determined separately for each of the standard lamps used.

F. ABSOLUTE SPECTRAL DISTRIBUTION OF THE SPHERE OUTPUT

The spherical integrator as a source of radiant flux has a different spectral configuration than that of an approximate point source such as the standard quartz-iodine lamp. In order to obtain an absolute calibration by comparing the spectral distribution of the sphere with that of the standard lamp it is necessary to eliminate the effects of this difference. Since "the role of a diffusely reflecting surface is to obliterate the past history of the incident radiation" (Ref. 18), a 16-inch spherical integrator was mounted on the front of the Perkin Elmer Monochromator. This small sphere consists of two plastic hemispherical shells painted with Burch sphere paint on the inside and aluminum paint on the outside. The two hemispheres are held together by means of clamps. One of the hemispheres was rigidly fastened to the monochromator so that a 1.8 cm diameter exit port was centered in front of the monochromator slit. The second hemisphere has a 3.7 cm diameter entrance port which is designed to be rotated alternately into a position (a) such that it may be positioned at the exit port of the six-foot integrator so that it is on the inside curvature of the six-foot integrator and thus receives flux from all parts of the large sphere, or (b) so as to be in line with the standard quartz-iodine lamp located at 20 cm from this port and thus receive the flux from the standard lamp. Using the small sphere in this way, the monochromator alternately saw the flux emitted by the six-foot integrator or from the standard lamp at 20 cm, after the flux was integrated by the small sphere.

Using a given slit width of the monochromator and gain of the recorder a direct comparison was made between the total flux which the small sphere received from the six-foot integrator and from the standard lamps which had been used to get the relative ratios as described above. This was done using the photomultiplier detector 1P28 at the following wavelengths: 0.45, 0.50, 0.53, 0.55, 0.60 microns. This procedure was repeated using the Reeder thermocouple detector at the following wavelengths: 0.6, 0.9, 1.0, 1.1, 1.2, 1.3 microns.

Let $D_{sa\lambda}$ be the recorder deflection of the monochromator at one of the above-mentioned wavelengths when the small sphere receives flux from the six-foot integrator, and $D_{1a\lambda}$ the deflection at the same wavelength when it receives flux from one of the standard lamps placed at 20 cm from the entrance port. Then $k_{a\lambda} = D_{sa\lambda}/D_{1a\lambda}$ is the absolute ratio of the flux from the six-foot integrator to that of the standard lamp at this wavelength. The absolute ratios for all wavelengths measured may be obtained by normalizing the relative ratios $k_{r\lambda}$ to these absolute ratios k_{a_λ}.

When the small sphere, mounted on the monochromator, has its entrance port located at the exit port of the six-foot integrator, the flux incident on the entrance port is obviously the same flux which is incident on the corresponding portion of the exit port of the six-foot integrator. Since this flux comes from all parts of the inside surface of the integrator by diffuse reflection, each elemental area of the inside surface of the small sphere receives flux from an equivalent fractional portion of the inside surface of the integrator which is on the line of sight through the port with that of the small sphere. This means that the small sphere receives completely diffuse radiation from the six-foot integrator.

In order to determine the total flux received by the small sphere, one must evaluate it in terms of the flux incident at the exit port of the integrator which has come from all parts of the diffusing surface of the integrator. Let $F_{s\lambda}$ watts $\cdot\ cm^{-2} \cdot \mu^{-1}$ be diffusely reflected into the solid angle 2π. Then the diffuse spectral radiation in the normal direction is $F_{s\lambda}/\pi$. The spectral radiant flux from the diffusely reflecting surface of the spherical segment of area dA_s which is incident at the effective area of the exit port, and hence of the area A of the entrance port of the small sphere is equal to

$$A\,dW_s = \frac{F_s}{\pi} \times \frac{dA_s \times \cos \tfrac{1}{2}\theta \times A \cos \tfrac{1}{2}\theta}{d^2} \tag{8}$$

where d is the distance between the element of area dA_s and the port, and $\frac{1}{2}\theta$ is the angle between the line of sight propagation from this area and the inner normal to the sphere at the same point on dA_s, as is shown in Figure 5. Since $d = 2r \cos \frac{1}{2}\theta$, and $dA_s = 2\pi r^2 \sin \theta \, d\theta$, the element of spectral radiant power at the entrance port of the small sphere is

$$dP_{s\lambda} = A \, dW_{s\lambda} = \frac{F_{s\lambda}}{\pi} \; \frac{2\pi r^2 \sin \theta \, d\theta \cos^2 \frac{1}{2}\theta \, A}{4 r^2 \cos^2 \frac{1}{2}\theta} . \qquad (9)$$

Upon simplification this becomes $dP_{s\lambda} = \frac{1}{2} F_{s\lambda} A \sin \theta \, d\theta$. Thus the spectral radiant power at the port of the six-foot integrator and hence at the entrance port of the small sphere is

$$P_{s\lambda} = \tfrac{1}{2} F_{s\lambda} A \int_0^{\theta} \sin \theta \, d\theta = \tfrac{1}{2} F_{s\lambda} A \, (1 - \cos \theta) . \qquad (10)$$

Since θ varies essentially from 0° to 180° because of the size of the port and the relative positions of the ports of the two spheres Equation (10) becomes

$$P_{s\lambda} = W_{s\lambda} A = F_{s\lambda} A \text{ watts/micron} . \qquad (11)$$

This diffuse flux from the six-foot integrator was integrated by the small sphere so that the radiant emittance at the exit port of the small sphere is given by Equation (7) as

$$W'_{s\lambda} = \frac{W_{s\lambda} A}{4\pi r_1^2} \times \frac{\rho_\lambda}{1 - \rho_\lambda} \qquad (12)$$

where r_1 is the radius of the small sphere and ρ_λ is the spectral reflectance of the sphere paint. This flux was viewed by the monochromator. The resulting recorder deflection $D_{sa\lambda}$ was proportional to the integrated flux $W'_{s\lambda}$ and hence to the spectral radiant emittance $W_{s\lambda}$ of the six-foot integrator.

On the other hand when the small sphere, mounted on the monochromator, receives flux from the standard lamp, it comes from approximately a point source. Let $J_{1\lambda}$ watts/steradian/micron be the spectral radiant intensity of

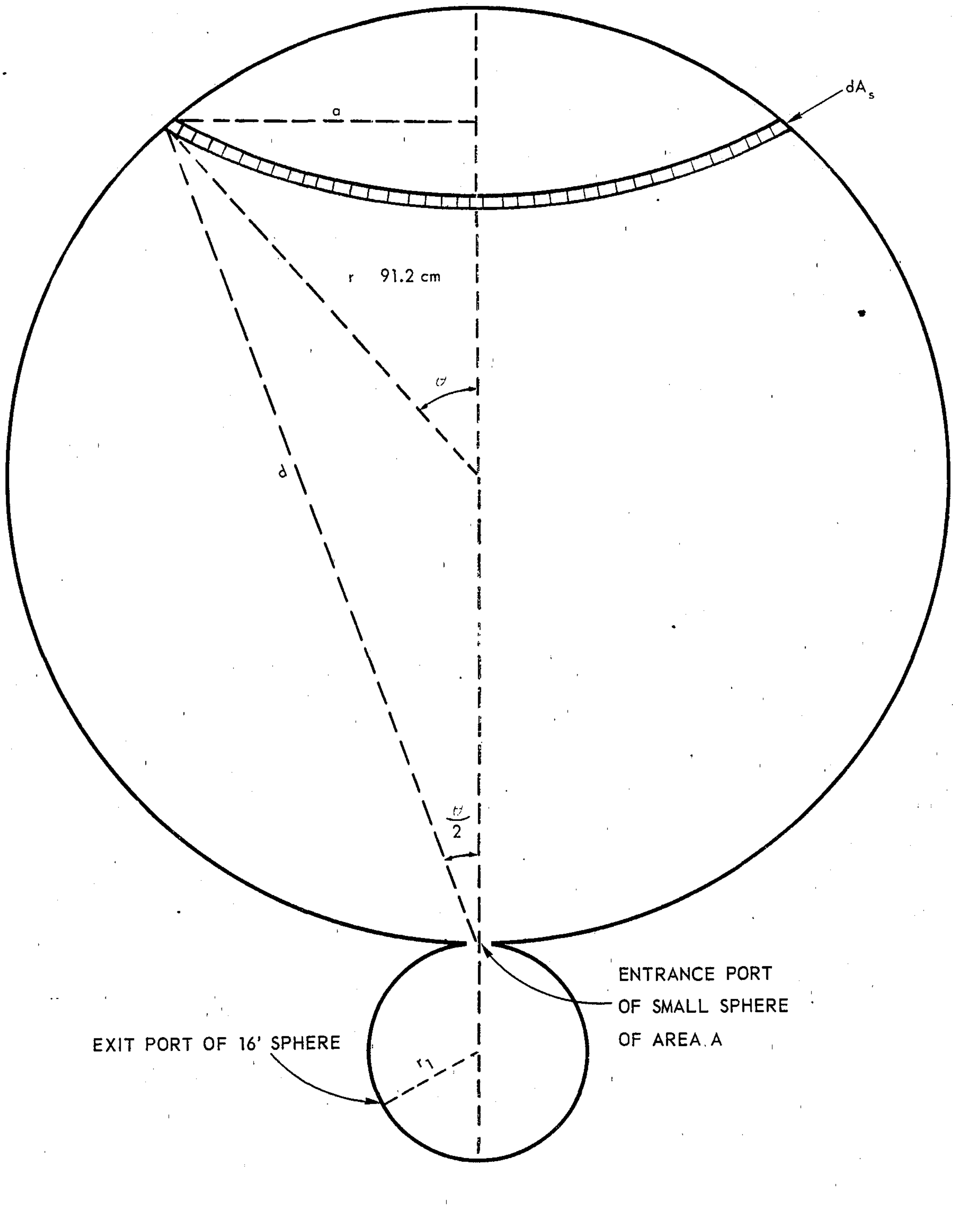

Figure 5. Cross Section of Large and Small Spheres Showing Geometrical Parameters for Deriving Radiance Equations

the standard quartz-iodine lamp. Then the spectral irradiance per unit area at the port of the small sphere due to the standard lamp at 20 cm is given by

$$H_{1\lambda} = CJ_{1\lambda}/r^2 \text{ watts/cm}^2\text{/micron.} \tag{13}$$

where $r = 20$ cm is the distance from the lamp to the entrance port and C is a correction factor to correct for inverse square failure. The spectral radiant power received by the small sphere from the standard lamp is given by

$$P_{1\lambda} = H_{1\lambda} A \text{ watts/micron} \tag{14}$$

where A is the area of the entrance port of the small sphere.

As mentioned previously, the flux received by the small sphere from the six-foot integrator is diffuse radiation. The flux from the standard lamp, however, comes from approximately a point source and falls on a relatively small area of the inside of the small sphere after which it is diffusely reflected. Thus the flux from the standard lamp only becomes comparable to the diffuse radiation received from the six-foot integrator after it has undergone a single diffuse reflection. Hence the effective radiant power from the standard lamp which will be integrated by the small sphere is obtained by multiplying Equation (14) by the spectral reflectance of the sphere paint ρ_λ so that

$$P'_{1\lambda} = \rho_\lambda \times H_{1\lambda} A \text{ watts/micron} \tag{15}$$

This correction was not made in the preliminary results reported previously (Ref. 19). This effective flux was integrated by the small sphere. Hence the spectral radiant emittance at the exit port of the small sphere which is viewed by the monochromator is found by Equation (7) to be

$$W_{1\lambda} = \frac{\rho_\lambda \times H_{1\lambda} A}{4\pi r_1^2} \times \frac{\rho_\lambda}{1 - \rho_\lambda} \text{ watts/cm}^2\text{/micron} \tag{16}$$

where r_1 is the radius of the small sphere. The corresponding recorder deflection $D_{1a\lambda}$ was proportional to the emittance $W_{1\lambda}$ and thus to the effective flux $\rho_\lambda \times H_{1\lambda}$ received from the lamp after a single diffuse reflection.

It is therefore possible to compare the spectral radiant emittance which the small sphere received from the six-foot integrator with the spectral intensity from the standard lamp after a single diffuse reflection in terms of the corresponding deflections of the recorder as seen by dividing Equation (12) by Equation (16), or

$$\frac{W'_{s\lambda}}{W_{1\lambda}'} = \frac{\dfrac{W_{s\lambda} A}{4\pi r_1^2} \times \dfrac{\rho_\lambda}{1 - \rho_\lambda}}{\dfrac{\rho_\lambda H_{1\lambda} A}{4\pi r_1^2} \times \dfrac{\rho_\lambda}{1 - \rho_\lambda}} = \frac{W_{s\lambda}}{\rho_\lambda H_{1\lambda}} . \tag{17}$$

As stated before, the monochromator deflections are proportional to the intensity of the flux seen by the monochromator if the gain and the slit width are held constant. Hence the absolute ratio of the recorder deflections is equal to the ratio given by Equation (17), or

$$k_{a\lambda} = D_{sa\lambda}/D_{1a\lambda} = W'_{s\lambda}/W_{1\lambda} = W_{s\lambda}/\rho_\lambda H_{1\lambda} .$$

Thus one obtains

$$W_{s\lambda} = \rho_\lambda H_{1\lambda} D_{sa\lambda}/D_{1a\lambda} \text{ watts/cm}^2\text{/micron} . \tag{18}$$

for the spectral radiant emittance of the six-foot integrator.

Using Equation (18) the diffuse spectral emittance of the six-foot integrator was calculated every tenth of a micron or less from 0.32 to 2.7 microns for each standard lamp separately. The resulting data in the case of standard lamp QM-95 is given in Table IV. The wavelength is in microns. The second column gives the spectral irradiance of the standard lamp QM-95 at 20 cm (in milliwatts/cm^2/micron). The third column gives the spectral radiance after a single reflection by the small sphere. The fourth column gives the absolute ratios of the recorder deflections. The fifth column gives the diffuse spectral radiant emittance of the six-foot integrator when twelve lamps are operating. Table V gives the mean spectral radiant emittance of the integrator as determined using the standard lamps QM-95, EPI-1154, and EPI-1155. Figure 6 shows the spectral distribution of the six-foot integrator as determined by the use of lamp QM-95, and also shows the spectral distribution of lamp QM-95.

Table IV

Spectral Radiant Emittance of Spherical Integrator

Determined By Use of Lamp QM-95

λ	H_λ	$\rho_\lambda H_\lambda$	$D_{s\lambda_a}/D_{e\lambda_a}$	$W_{s\lambda}$
.32	2.202	1.381	.0967	.1335
.35	5.058	3.566	.2059	.7343
.37	7.831	5.915	.3352	1.983
.40	13.63	10.93	.5713	6.246
.45	27.19	22.95	.9023	20.71
.50	45.45	39.72	1.203	47.79
.55	66.01	58.81	1.457	85.68
.60	87.60	79.10	1.748	138.2
.65	108.0	98.45	1.781	175.3
.70	124.6	113.9	1.810	206.1
.75	136.9	125.0	1.883	235.5
.80	144.3	131.8	1.965	259.0
.90	149.9	136.4	1.777	242.4
1.00	146.8	132.7	1.562	207.4
1.1	138.2	123.7	1.378	170.4
1.2	126.4	110.9	1.197	132.8
1.3	114.1	99.29	1.082	107.4
1.4	101.8	83.97	.5685	47.74
1.5	90.06	72.59	.5604	40.68
1.6	78.96	63.40	.5701	36.15
1.7	69.09	52.23	.3925	20.50
1.8	60.01	44.41	.2988	13.27
1.9	51.94	36.25	.1877	6.806
2.0	44.91	28.96	.1851	5.362
2.1	39.23	25.27	.1921	4.853
2.2	34.67	22.67	.1792	4.064
2.3	30.89	19.93	.1062	1.798
2.4	27.88	13.66	.07856	1.073
2.5	25.54	11.75	.05798	.6811
2.6	19.84	8.790	.03022	.2656
2.7	17.41	5.067	.03016	.1528

Table V

Spectral Radiant Emittance of Six-Foot Spherical Integrator

(λ in microns; W_λ in milliwatts $\cdot$ cm^{-2} $\cdot$ μ^{-1})

λ	W_λ	λ	W_λ
		1.1	170
.32	.136	1.2	132
.35	.745	1.3	106
.37	1.99	1.4	48.0
.40	6.24	1.5	40.7
.45	20.3	1.6	36.5
.50	47.3	1.7	20.6
.55	84.8	1.8	13.1
.60	139	1.9	6.82
.65	176	2.0	5.32
.70	204	2.1	4.77
.75	237	2.2	3.92
.80	263	2.3	1.73
.90	249	2.4	1.05
1.00	209	2.5	.665
		2.6	.252
		2.7	.140

G. ANALYSIS OF RESULTS

An examination of the spectral curves in Figure 6 reveals several significant facts. First, it will be observed that the peak value of the integrator emittance is 1.73 times the peak value of the irradiance of the standard lamp at 20 cm. Secondly, the maximum intensity of the integrator emittance is located at approximately 0.82 micron while the maximum value of the irradiance of the standard lamp is located at approximately 0.92 micron. Thirdly, for those wavelengths for which the reflectance of the sphere paint is high, the sphere amplifies the emitted power, while for the wavelengths for which the reflectance is low, the emitted power of the sphere is less than that of the source.

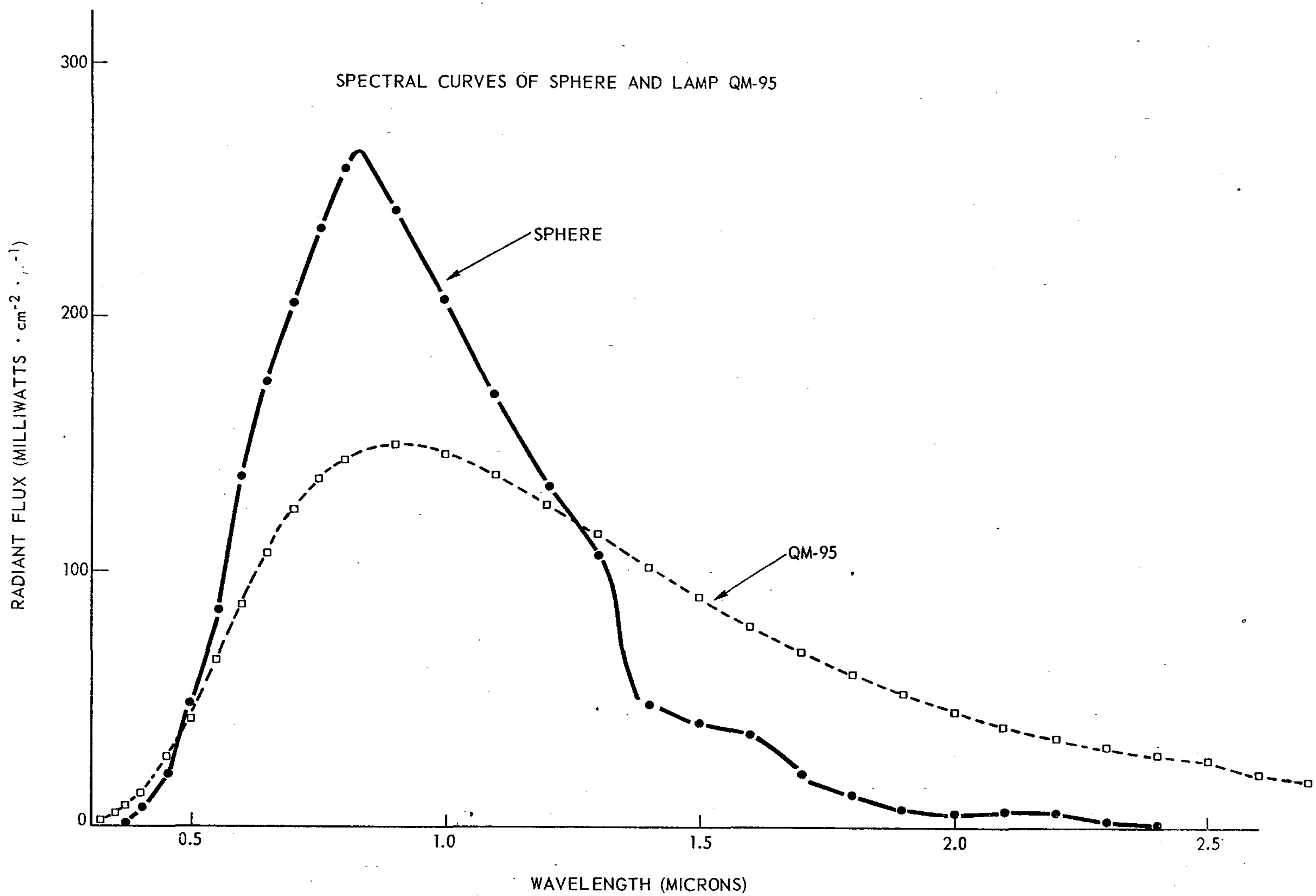

Figure 6. Spectral Radiant Emittance of Six-Foot Spherical Integrator and of One Standard Lamp #QM-95

A comparison of the spectral distribution of the integrator emittance as determined by the three standard lamps shows that the results are reasonably consistent. The greatest difference at a given wavelength between the three sets of data is usually less than three percent. At a few points the difference is as large as 6 percent. The National Bureau of Standards reports that the calibration of the standard lamps has an uncertainty of 8% in the ultraviolet and one of 3% in the visible and the infrared (Ref. 7). The data for the calibration of the sphere which was obtained by the use of the three standard lamps differ by the same order of magnitude.

There are a number of possible sources of error. First, there is some uncertainty in the reflectance of the sphere paint. The recording on the chart may be read to within 0.5%. In reversing the two samples of freshly smoked MgO in the Cary 14 spectrophotometer while determining the reflectance of the Burch sphere paint, the difference in reflectance was found to be less than 0.5% at most points. The data for the reflectance of MgO which has been reported by various observers differ somewhat. It seems to depend on the nature of the surface, the thickness of the layer and the age. The reported uncertainty in the reflectance of the MgO standard is less than 1% in the spectral range where the quartz-iodine lamp is most intense, while in the near infrared this uncertainty may be as high as 5%.

Secondly, there is a variation in the voltage across the 200-watt lamps in the integrator. This variation has been found to be 1% or less in the case of the eight lamps operated by two of the power supplies, and has been as high as 2% in the lamps operated by the third power supply. This would represent a variation in the flux of the lamps and hence of the sphere of about two percent in the case of eight lamps and one of up to 4% in the case of lamps 9 to 12.

Among other sources of error may be mentioned the monochromator slit which may be set within 0.2%. The chart which records the magnitude of the flux at various wavelengths can be read within 0.5%. It has been observed that there is a decrease in a 0.1 microvolt test signal as shown by the corresponding recorder deflections at the beginning and the end of a run. This change at times was as high as 5 or 6%. If this change is due to non-constancy of the amplifier, the data obtained for the spectral distribution of the sphere and of the standard lamps may vary by a similar amount. Since the three lamps were used independently and since the differences in the resulting data show a random variation, some of these errors may compensate each other. Thus the over-all uncertainty of the data may be of the order of 5% or less. This is about the same as the difference between the values of the integrator emittance as obtained by means of the three standard lamps.

In comparing the calibration reported here with the calibration which was reported in 1964 (Ref. 17) it is observed that the present values of the spectral emittance of the sphere are about 30% greater than previously. This change is supported by the response of a thermopile to the energy emitted by the sphere. In comparing the response of thermopile 4928A to the present flux with its response in 1964, it is found that the present flux gives an output voltage which is 39.6% greater than previously. This increase may be due in part to the fact that the sphere was repainted and also to the fact that the lamps were previously at 29.8 volts while at present they are operated at 6.5 amperes (or about 30.3 volts). It would seem that these factors might contribute to this increase by at most several percent. More important as a factor in this increase may be the relocation of the lamps in the sphere.

IV. CONCLUSIONS

Several small area energy sources were found to be useful laboratory calibration sources. These include the blackbody, the quartz-iodine lamp, the strip filament lamp, and a tungsten lamp being used to replace the carbon filament lamp.

The blackbody is obviously the ideal small area source, since the radiant energy may be determined provided its temperature, aperture, and emissivity are known. The two blackbodies which were used in this laboratory had a maximum operating temperature of 1000°C. It was found that it would have been desirable to have an operating temperature which is considerable higher than this for some of our applications. It also became clear that a completely satisfactory blackbody must be provided with a means of maintaining the face plate (and aperture) at ambient temperature.

Although the blackbody is the ideal small area energy source, it has proved to be much more convenient to use the tungsten strip filament lamp or the more recently developed quartz-iodine lamp for normal use as small area sources of spectral irradiance. The irradiance of these lamps has been determined directly or indirectly by comparison with the blackbody. Since the N.B.S. calibration covers only the spectral range from 0.25 to 2.6 microns, it was found desirable to extend this calibration to 4.8 microns in the case of the tungsten strip filament lamp and the quartz-iodine lamps by methods described above. Future plans call for an extension of the spectral irradiance calibration toward shorter wavelengths for use in the vacuum ultraviolet.

For some applications, it is necessary to use a standard of total irradiance. While the blackbody would be the ideal source of total irradiance, the new tungsten filament lamp is more convenient and provides a great improvement over the long used carbon filament lamp. The new lamp has a color temperature of the order of 2700-2850°K as compared to 1800°K for the carbon filament thus providing a much greater source of radiant energy.

A method has been described above which was used to evaluate the total irradiance of the tungsten strip filament and quartz-iodine standards of spectral irradiance. In the case of the quartz-iodine lamp for example, the total evaluated irradiance differs by less than 2% from the total energy input into the lamp. Thus the accuracy of this evaluation is apparently comparable to the accuracy claimed by the N.B.S. for the standards of spectral irradiance, or 3% in the visible and near infrared and 8% at the shortest wavelengths in the ultraviolet. It is of interest to note in this connection that the average response of an Eppley water-cooled thermopile to three 1000-watt quartz-iodine lamps evaluated for total irradiance by the method described above, differs by less than two percent from the response to a 1000-watt standard of total irradiance.

The present arrangement of the Six-Foot Spherical Integrator apparently provides a satisfactory extended source for the calibration of detectors in the visible and near infrared. The uncertainty of the calibration is estimated to be at most five percent. Work is under way to test this by comparing the calibration of radiometers obtained with the present set-up and that which was obtained previously by other methods.

REFERENCES

1. Earl B. Brown, Modern Optics, New York, Reinhold, 1965, p. 33.

2. Ralph Stair, Russel G. Johnston and W. W. Halbach, Journal of Research of the National Bureau of Standards, Vol. 64, p. 291, 1960.

3. Mark Pivovonsky and Max R. Nagel, Tables of Blackbody Radiation Functions, New York, MacMillan, 1961.

4. J. C. de Vos, Physica, Vol. 20, p. 690, 1954.

5. E. G. Zubler and F. A. Mosby, Illumination Engineering, Vol. 54, p. 734, 1959.

6. J. A. Moore and C. M. Jolly, General Electric Company Journal, Vol. 29, p. 99, 1962.

7. R. Stair, W. E. Schneider and J. K. Jackson, Applied Optics, Vol. 2, p. 1151, 1963.

8. GSFC Final Report of the Workshop Program 1965, p. B-39.

9. M. Pirani, Journal of Scientific Instruments, Vol. 16, p. 372, 1939.

10. R. J. P. Lyon, NASA Contract Report, NASA CR-100, Nov. 1964.

11. Howard O. McMahon, Journal of the American Ceramic Society, Vol. 34, p. 91, 1951.

12. Ralph Stair, William E. Schneider and William B. Fussell, Applied Optics, Vol. 6, p. 101, 1967.

13. GSFC Final Report of the Workshop Program 1965, p. B-47.

14. W. E. Sumpner, Physics Society Proceedings, Vol. 12, p. 10, 1892.

15. J. W. T. Walsh, Photometry, London, Constable and Co., 1958, p. 258.

16. A. C. Hardy and O. W. Pineo, Journal of the Optical Society of America, Vol. 21, p. 502, 1931.

17. GSFC Final Report of the Workshop Program 1964, p. A-17.

18. E. M. Sparrow and R. D. Cess, Radiation Heat Transfer, Belmont, Calif., Brooks/Cole Pub. Co., 1966, p. 52.

19. GSFC Final Report of the Workshop Program 1966, p. 399.